Light cone wave functions in the context of space like transition form factors and prompt hadroproduction of $\eta_c\,(1S,\,2S)$

Izabela Babiarz

The Henryk Niewodniczański Institute of Nuclear Physics
Polish Academy of Sciences, Kraków

XIV International Conference on Beauty, Charm and Hyperon Hadrons - BEACH 2022
Kraków, 10^{th} June, 2022

THE HENRYK NIEWODNICZAŃSKI
INSTITUTE OF NUCLEAR PHYSICS
POLISH ACADEMY OF SCIENCES

POLISH NATIONAL AGENCY
FOR ACADEMIC EXCHANGE

Contents

Introduction

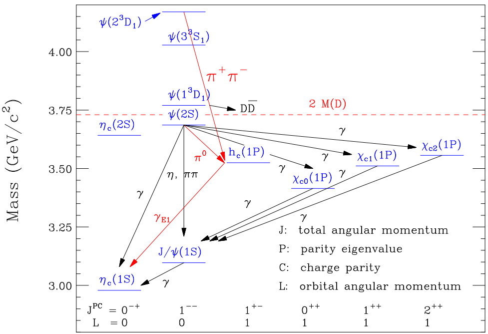

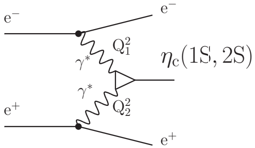

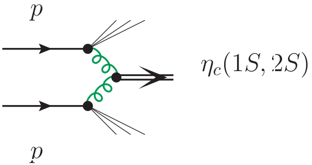

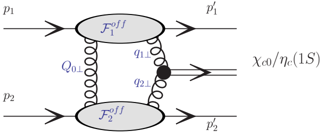

- Charmonia with even charge parity ($c\bar{c}$ states) : prompt production via gluon-gluon fusion.
- Quarkonia can provide a good test for unintegrated gluon densities.

Description of the mechanism $\gamma^*\gamma^* \to \eta_c(1S, 2S)$

Production of η_c in the double-tagged mode of e^+e^- collisions measures the $\gamma^*\gamma^* \to \eta_c(1S, 2S)$ transition form factor.

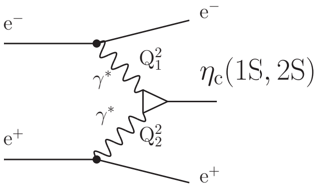

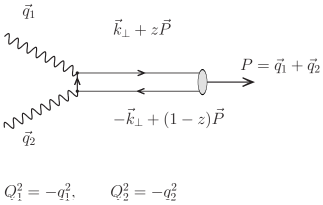

$$\mathcal{M}_{\mu\nu}(\gamma^*(q_1)\gamma^*(q_2) \to \eta_c) = 4\pi\alpha_{\rm em}\,(-i)\varepsilon_{\mu\nu\alpha\beta}q_1^\alpha q_2^\beta\, F(Q_1^2, Q_2^2)$$

The light-cone representation of the transition form factor:

$$F(Q_1^2, Q_2^2) = e_c^2\sqrt{N_c}4m_c \cdot \int \frac{dz d^2\mathbf{k}}{z(1-z)16\pi^3}\psi(z,\mathbf{k})$$
$$\times \left\{ \frac{1-z}{(\mathbf{k}-(1-z)\mathbf{q}_2)^2 + z(1-z)\mathbf{q}_1^2 + m_c^2} + \frac{z}{(\mathbf{k}+z\mathbf{q}_2)^2 + z(1-z)\mathbf{q}_1^2 + m_c^2} \right\}.$$

$$Q_i^2 = \mathbf{q}_i\,,\ \vec{k_\perp} \equiv \mathbf{k}$$

I.Babiarz, V.P.Goncalves, R.Pasechnik, W.Schäfer, andA.Szczurek
Phys.Rev.D 100 (2019) 5, 054018

The construction of the $\gamma^*\gamma^* \to \eta_c$ form factor

The general form of the amplitude $\Rightarrow$ the invariant form factor:

$$\frac{1}{4\pi\alpha_{\rm em}}\mathcal{M}_{\mu\nu}(\gamma^*(q_1)\gamma^*(q_2) \to \eta_c) = (-i)\varepsilon_{\mu\nu\alpha\beta}q_1^\alpha q_2^\beta F(Q_1^2, Q_2^2)$$

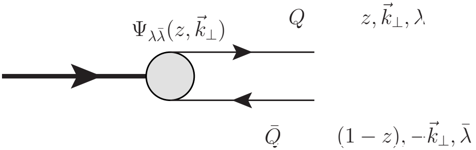

$$\mathbf{p}_Q = \vec{k}_\perp + z\vec{P}_\perp$$
$$\mathbf{p}_{\bar{Q}} = -\vec{k}_\perp + (1-z)\vec{P}_\perp$$

Frame-independent $Q\bar{Q}$ component from LF-Fock-state expansion:

$$|\mathrm{Meson}; P_+, \vec{P}_\perp\rangle =$$
$$\sum_{i,j,\lambda,\bar{\lambda}} \frac{\delta^i_j}{\sqrt{N_c}} \int \frac{dzd^2\vec{k}_\perp}{z(1-z)16\pi^3}\Psi_{\lambda\bar{\lambda}}(z, \vec{k}_\perp)|Q_{i\lambda}(zP_+, \mathbf{p}_Q)\bar{Q}^j_{\bar{\lambda}}((1-z)P_+, \mathbf{p}_{\bar{Q}})\rangle + \dots$$

$Q\bar{Q}$ interaction potential model

$$\frac{\partial^2 u(r)}{\partial r^2} = (V_{\text{eff}}(r) - \epsilon)u(r), \quad u(r) = rR(r), \epsilon = m_Q E, \quad V_{eff} = m_Q V(r) + \frac{\ell(\ell+1)}{r^2}$$

$Q\bar{Q}$ interaction potential models:

1. **Buchmüller-Tye**, $m_c = 1.48\,\mathrm{GeV}$, $m_b = 4.87\,\mathrm{GeV}$,
   $V(r) =$
   $$\begin{cases} \frac{k}{r} - \frac{8\pi}{27}\frac{v(\lambda r)}{r}, & r \geq 0.01 fm \\ \frac{-16\pi}{25}\frac{1}{r\ln(w(r))}\left(1 + 2(\gamma_E + \frac{53}{75})\frac{1}{\ln w(r)} - \frac{462}{625}\frac{\ln\ln(w(r))}{\ln(w(r))}\right), & \leq 0.01 fm \end{cases}$$
2. **Cornell**, $m_c = 1.84\,\mathrm{GeV}$, $m_b = 5.17\,\mathrm{GeV}$, $V(r) = \frac{-k}{r} + \frac{r}{a^2}$
3. **logarithmic**, $m_c = 1.5\,\mathrm{GeV}$, $m_b = 5.0\,\mathrm{GeV}$,
   $V(r) = 0.6635\,\mathrm{GeV} + (0.733\,\mathrm{GeV})\log(r \cdot 1\,\mathrm{GeV})$
4. **harmonic oscillator** $m_c = 1.4\,\mathrm{GeV}$, $m_b = 4.2\,\mathrm{GeV}$, $V(r) = \frac{1}{4}m_Q\omega^2 r^2$
5. **power-like**, $m_c = 1.334\,\mathrm{GeV}$ $V(r) = 6.41\mathrm{GeV} + (6.08\mathrm{GeV})(r \cdot 1\mathrm{GeV})^{0.106}$

Nonrelativistic quarkonium wave functions

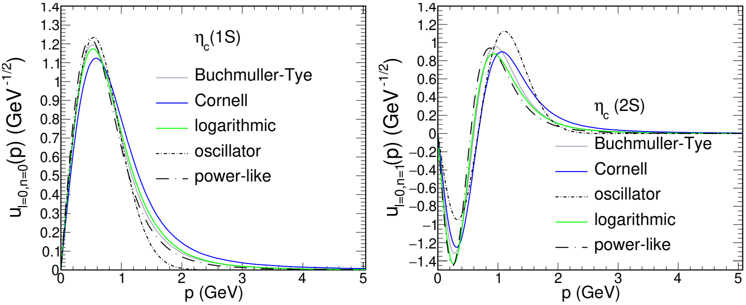

Figure: Radial momentum space wave function for different potentials.

Radial space wave function are obtained from the Schrödinger equation

$$\frac{\partial^2 u(r)}{\partial r^2} = (V_{\rm eff}(r) - \epsilon)u(r), \qquad u(r) = rR(r) \quad , \epsilon = m_Q E, \quad V_{eff} = m_Q V(r) + \frac{l(l+1)}{r^2}$$

$$\int\limits_0^\infty |u(r)|^2 dr = 1 \quad \Rightarrow \quad u(p) = \sqrt{\frac{2}{\pi}} \int_0^\infty \sin(p\, r) u_{00}(r)\, dr$$

Light-cone wave functions from rest-frame - Terentev prescription

Rest-frame wave functions for $J = 0$:

$$\Psi_{\tau\bar{\tau}}(\vec{p}) = \underbrace{\frac{1}{\sqrt{2}}\xi_Q^{\tau\dagger}\,\hat{\mathcal{O}} i\sigma_2\,\xi_{\bar{Q}}^{\bar{\tau}*}}_{\text{spin}-\text{orbit}}\underbrace{\frac{u(p)}{p}}_{\text{radial}}\frac{1}{\sqrt{4\pi}};$$

$$\text{where } \hat{\mathcal{O}} = \begin{cases} \mathbb{I} & \text{spin-singlet, } S=0, L=0. \\ \frac{\vec{\sigma}\cdot\vec{k}}{k}, & \text{spin-triplet, } S=1, L=1. \end{cases}$$

mapping RF momentum to LC representation:

$$\vec{p} = (\vec{k}_\perp, k_z) = (\vec{k}_\perp, \frac{1}{2}(2z-1)M_{c\bar{c}}),\; M_{c\bar{c}}^2 = \frac{\vec{k}_\perp^{\,2} + m_Q^2}{z(1-z)},$$

$$\psi(z, \vec{k}_\perp) = \frac{\pi}{\sqrt{2M_{c\bar{c}}}}\frac{u(p)}{p}\,.$$

Light-cone wave functions from rest-frame - Melosh-transformation

Melosh-transf. of spin-orbit part:

$$\xi_Q = R(z, \vec{k}_\perp)\chi_Q, \quad \xi^*_{\bar{Q}} = R^*(1-z, -\vec{k}_\perp)\chi^*_{\bar{Q}}\,,$$

$$R(z, \vec{k}_\perp) = \frac{m_Q + zM - i\vec{\sigma}\cdot(\vec{n}\times\vec{k}_\perp)}{\sqrt{(m_Q + zM)^2 + \vec{k}_\perp^{\,2}}}$$

$$\hat{\mathcal{O}}' = R^\dagger(z, \vec{k}_\perp)\mathcal{O}\, i\sigma_2 R^*(1-z, -\vec{k}_\perp)(i\sigma_2)^{-1}$$

using properties of Pauli-matrices $i\sigma_2\vec{\sigma}^*(i\sigma_2)^{-1} = -\vec{\sigma}$

$$\hat{\mathcal{O}}' = R^\dagger(z, \vec{k}_\perp)\hat{\mathcal{O}}\, R(1-z, -\vec{k}_\perp)\,.$$

Light-front wave functions

Pseudoscalar (S-wave)

$$
\begin{aligned}
\Psi_{\lambda\bar{\lambda}}(z,\vec{k}_\perp) &= \begin{pmatrix} \Psi_{++}(z,\vec{k}_\perp) & \Psi_{+-}(z,\vec{k}_\perp) \\ \Psi_{-+}(z,\vec{k}_\perp) & \Psi_{--}(z,\vec{k}_\perp) \end{pmatrix} \\
&= \frac{1}{\sqrt{z(1-z)}} \begin{pmatrix} -k_x + ik_y & m_Q \\ -m_Q & -k_x - ik_y \end{pmatrix} \psi(z,\vec{k}_\perp)
\end{aligned}
$$

Normalisation

$$
\begin{aligned}
1 = \int_0^1 \frac{\mathrm{d}z}{z(1-z)} \int \frac{\mathrm{d}^2\vec{k}_\perp}{16\pi^3} \sum_{\lambda\bar{\lambda}} |\Psi_{\lambda\bar{\lambda}}(z,\vec{k}_\perp)|^2 \\
= \int_0^1 \frac{\mathrm{d}z}{z(1-z)} \int \frac{\mathrm{d}^2\vec{k}_\perp}{16\pi^3} 2M_{c\bar{c}}\psi(z,\vec{k}_\perp)
\end{aligned}
$$

Light-cone wave function for Buchmüller -Tye potential model

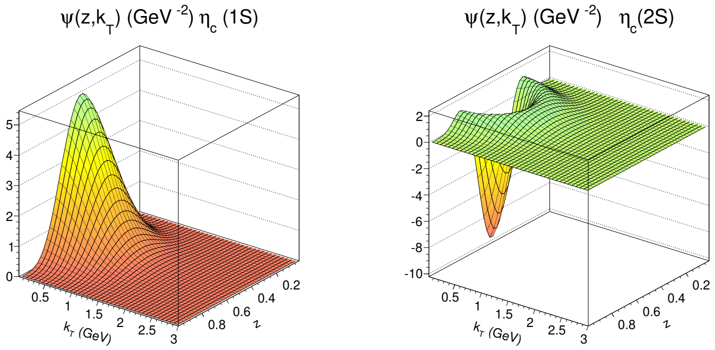

Figure: The light-front wave function $\psi(z, \vec{k}_\perp)$ for Buchmüller-Tye potential.

$F(0,0)$ transition for both on-shell photons

$$F(0,0) = e_c^2 \sqrt{N_c}\, 4m_c \cdot \int \frac{dz d^2\vec{k}_\perp}{z(1-z)16\pi^3} \frac{\psi(z,\vec{k}_\perp)}{\vec{k}_\perp^2 + m_c^2} \,,$$

$F(0,0)$ is related to the two-photon decay width by the formula:

$$\Gamma(\eta_c \to \gamma\gamma) = \frac{\pi}{4} \alpha_{\rm em}^2 M_{\eta_c}^3 \,|F(0,0)|^2 \,.$$

$F(0,0)$ can be rewrite in the terms of radial momentum space wave function $u(k)$:

$$F(0,0) = e_c^2 \sqrt{2N_c}\, \frac{2m_c}{\pi} \int_0^\infty \frac{dp\, p\, u(p)}{\sqrt{M_{c\bar{c}}^3}(p^2 + m_c^2)} \frac{1}{2\beta} \log\left(\frac{1+\beta}{1-\beta}\right) \,,$$

In the non-relativistic (NR) limit, where $p^2/m_c^2 \ll 1, \beta \ll 1$, and $2m_c \propto M_{c\bar{c}} \propto M_{\eta_c}$, we obtain

$$F(0,0) = e_c^2 \sqrt{N_c}\sqrt{2} \frac{4}{\pi\sqrt{M_{\eta_c}^5}} \int_0^\infty dp\, p\, u(p) = e_c^2 \sqrt{N_c} \frac{4\, R(0)}{\sqrt{\pi M_{\eta_c}^5}} \,,$$

where $\beta = \frac{p}{\sqrt{p^2+m_c^2}}$, the velocity v/c of the quark in the $c\bar{c}$ cms-frame and R(0) radial wave function at the origin.

$F(0,0)$ for both on-shell photons

Transition form factor $|F(0,0)|$ for $\eta_c(1S)$ at $Q_1^2 = Q_2^2 = 0$.

potential type	m_c [GeV]	$\vert F(0,0)\vert$ [GeV^{-1}]	$\Gamma_{\gamma\gamma}$ [keV]	f_{η_c}[GeV]
harmonic oscillator	1.4	0.051	2.89	0.2757
logarithmic	1.5	0.052	2.95	0.3373
power-like	1.334	0.059	3.87	0.3074
Cornell	1.84	0.039	1.69	0.3726
Buchmüller-Tye	1.48	0.052	2.95	0.3276
experiment	-	0.067 ± 0.003 [1]	5.1 ± 0.4 [1]	0.335 ± 0.075 [2]

[1] M. Tanabashi *et al.* [Particle Data Group], Phys. Rev. D **98**, no.3, 030001 (2018).

[2] K. W. Edwards *et al.* [CLEO Collaboration], Phys. Rev. Lett. **86**, 30 (2001) [hep-ex/0007012].

R(0) and $\gamma\gamma$-width for $\eta_c(1S)$ derived in **the non-relativistic limit**.

potential type	R(0)[GeV$^{3/2}$]	$\Gamma_{\gamma\gamma}$ [keV] $\mathrm{M} = \mathrm{M}_{\eta_c}$	$\Gamma_{\gamma\gamma}$ [keV] $\mathrm{M} = 2\mathrm{m_c}$
harmonic oscillator	0.6044	5.1848	5.8815
logarithmic	0.8919	11.290	11.157
power-like	0.7620	8.2412	10.297
Cornell	1.2065	20.660	13.568
Buchmüller-Tye	0.8899	11.240	11.409

$$f_{\eta_c}\varphi(z,\mu_0^2) = \frac{1}{z(1-z)}\frac{\sqrt{N_c}\,4m_c}{16\pi^3}\int d^2\mathbf{k}\,\theta(\mu_0^2 - \mathbf{k}^2)\,\psi(z,\mathbf{k}) \text{ and } \int_0^1 \mathrm{d}z\,\varphi(z,\mu_0^2) = 1$$

$F(0,0)$ for both on-shell photons

Transition form factor $|F(0,0)|$ for $\eta_c(2S)$ at $Q_1^2 = Q_2^2 = 0$.

potential type	m_c [GeV]	$\lvert F(0,0)\rvert$ [GeV^{-1}]	$\Gamma_{\gamma\gamma}$ [keV]	f_{η_c} [GeV]
harmonic oscillator	1.4	0.03492	2.454	0.2530
logarithmic	1.5	0.02403	1.162	0.1970
power-like	1.334	0.02775	1.549	0.1851
Cornell	1.84	0.02159	0.938	0.2490
Buchmüller-Tye	1.48	0.02687	1.453	0.2149
experiment [1]	-	0.03266 ± 0.01209	2.147 ± 1.589	

[1] M. Tanabashi *et al.* [Particle Data Group], Phys. Rev. D **98**, no.3, 030001 (2018).

R(0) and $\gamma\gamma$-width for $\eta_c(2S)$ derived in the **non-relativistic limit.**

potential type	R(0) [GeV$^{3/2}$]	$\Gamma_{\gamma\gamma}$ [keV] $\mathrm{M} = \mathrm{M}_{\eta_c}$	$\Gamma_{\gamma\gamma}$ [keV] $\mathrm{M} = 2\mathrm{m_c}$
harmonic oscillator	0.7402	5.2284	8.8214
logarithmic	0.6372	3.8745	5.6946
power-like	0.5699	3.0993	5.7594
Cornell	0.9633	8.8550	8.6493
Buchmüller-Tye	0.7185	4.9263	7.4374

Normalised transition form factor $F(Q^2, 0)/F(0, 0)$

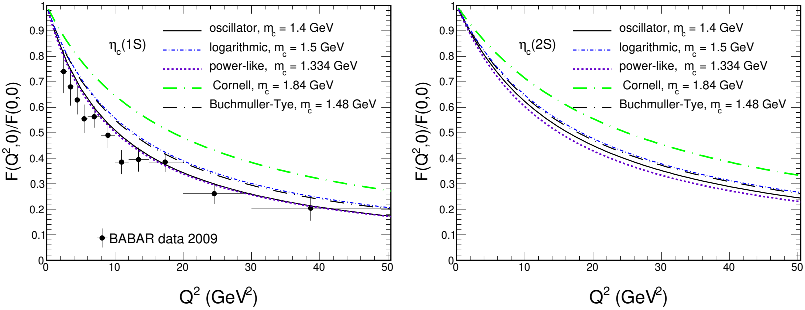

Figure: Normalised transition form factor $F(Q^2, 0)/F(0, 0)$ as a function of photon virtuality Q^2 (I. Babiarz et al.Phys.Rev.D 100 (2019) 5, 054018). The BaBar data are shown for comparison (J. P. Lees *et al.* [BaBar Collaboration], Phys. Rev. D **81**, 052010 (2010) [arXiv:1002.3000 [hep-ex]]).

Transition form factor $F(Q_1^2, Q_2^2)\,\gamma^*\gamma^* \to \eta_c(1S, 2S)$

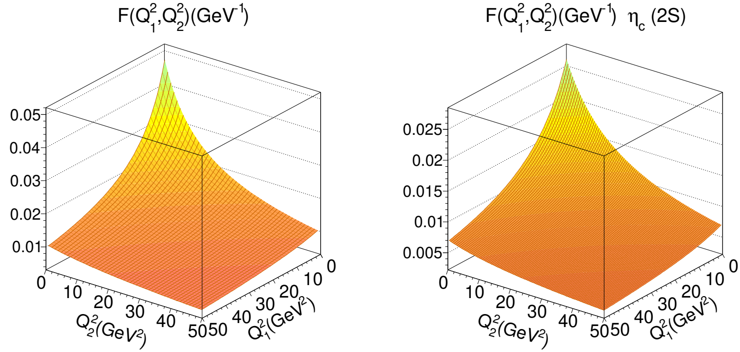

Figure: Transition form factor for $\eta_c(1S)$ and $\eta_c(2S)$ for Buchmüller -Tye potential. The sign of Bose symmetry Q_1^2, Q_2^2.

Transition form factor $F(\omega, \overline{Q^2})$

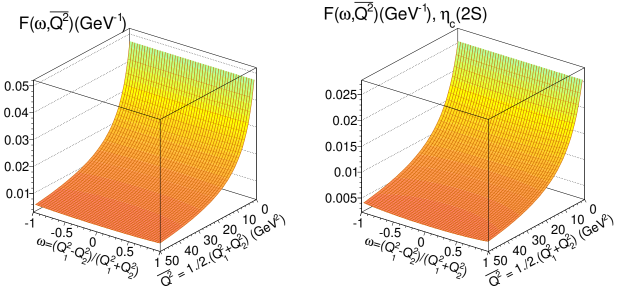

Figure: The $\gamma^*\gamma^* \to \eta_c$ (1S) and $\gamma^*\gamma^* \to \eta_c$ (2S) form factor as a function of (Q_1^2, Q_2^2) and $(\omega, \bar{Q}^2)$ for the Buchmüller-Tye potential for illustration.

$$\omega = \frac{Q_1^2 - Q_2^2}{Q_1^2 + Q_2^2} \quad \text{and} \quad \bar{Q}^2 = \frac{Q_1^2 + Q_2^2}{2} \, .$$

Asymptotic behaviour of $Q^2F(Q^2,0)$

The rate of approaching of $Q^2F(Q^2,0)$ to its asymptotic value predicted by Brodsky and Lepage G. P. Lepage and S. J. Brodsky, Phys. Rev. D **22**, 2157 (1980).
$Q^2F(Q^2,0) \to \frac{8}{3}f_{\eta_c}$, while $Q^2 \to \infty$

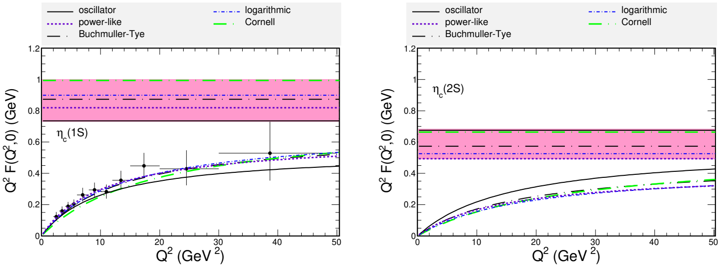

Figure: $Q^2F(Q^2,0)$ as a function of photon virtuality Q^2.Therefore the horizontal lines $\frac{8}{3}f_{\eta_c}$ are shown for reference.

Distribution amplitudes and quarkonium wave functions

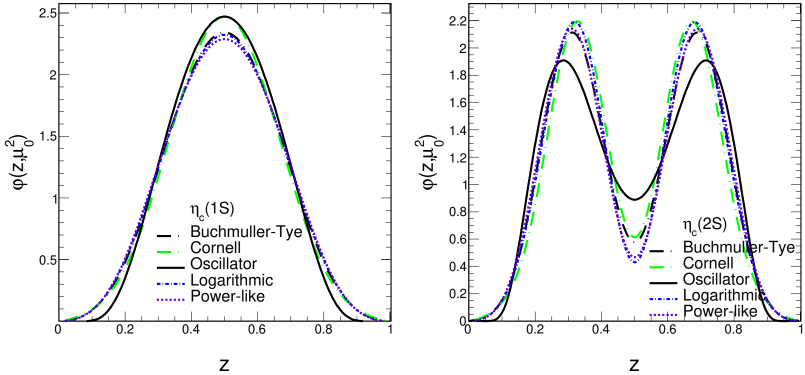

Figure: Distribution amplitudes for different wave functions for η_c (1S) (left panel) and for η_c (2S) (right panel).

$$f_{\eta_c}\varphi(z,\mu_0^2) = \frac{1}{z(1-z)}\int d^2\vec{k}_\perp\,\theta(\mu_0^2-\vec{k}_\perp^2)\,\psi(z,\vec{k}_\perp)$$

The evolution of the distribution amplitudes

Thanks of the Gegenbauer $C_n^{3/2}$ polynomials we can expand the distribution amplitudes:

$$\varphi(z,\mu^2) = 6z(1-z)\left(1 + a_2(\mu^2)C_2^{3/2}(2z-1) + \ldots\right) \ ,$$

and then extract the coefficients:

$$a_n(\mu_0) = \frac{2(2n+3)}{3(n+1)(n+2)} \cdot \int_0^1 dz \varphi(z,\mu_0) C_n^{3/2}(2z-1) \, ,$$

$$a_n(\mu) = a_n(\mu_0) \cdot \left[\frac{\alpha_s(\mu)}{\alpha_s(\mu_0)}\right]^{\gamma_n/\beta_0} \ .$$

with the anomalous dimensions γ_n, which can be found for example in *Phys.Rev.D 22 (1980) 2157*

$$\gamma_n = C_F\left(1 - \frac{2}{(n+1)(2+n)} + 4\sum_{m=2}^{n+1}\frac{1}{m}\right), \quad \beta_0 = \frac{11}{3}N_c - \frac{2}{3}N_f \ .$$

The evolution of the distribution amplitudes

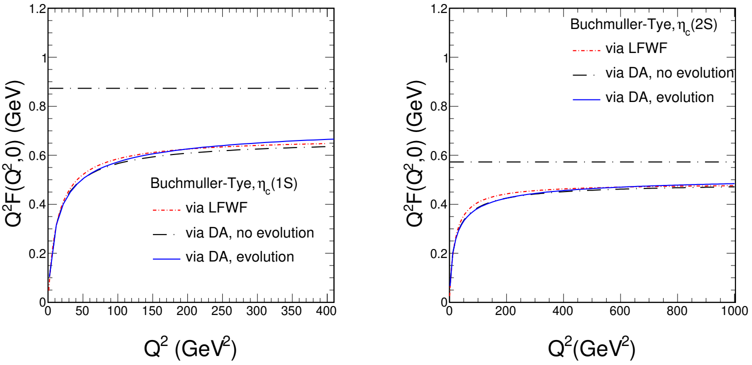

Figure: $Q^2F(Q^2)$ for η_c (1S)(left panel) and η_c (2S) (right panel) as a function of photon virtuality. The horizontal line is the limit for $Q^2 \to \infty$, calculated for the Buchmüller-Tye potential.

Hadroproduction of $\eta_c(1S,2S)$ via gluon-gluon fusion

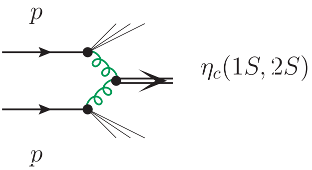

To the lowest order, it is proportional to the matrix element for the $\gamma^*\gamma^* \to \eta_c$ vertex. The form factor $\mathbf{I}(\vec{q}_{\perp 1}^{\,2}, \vec{q}_{\perp 2}^{\,2})$ is related to the $\gamma^*\gamma^* \to \eta_c$ transition form factor $F(Q_1^2, Q_2^2)$, $Q_i^2 = \vec{q}_{\perp i}^{\,2}$ as

$$\mathbf{F(Q_1^2, Q_2^2) = e_c^2\sqrt{N_c}\, I(\vec{q}_{\perp 1}^{\,2}, \vec{q}_{\perp 2}^{\,2})}$$

$$\frac{d\sigma}{dy d^2\vec{p}_\perp} = \int \frac{d^2\vec{q}_{\perp 1}}{\pi \vec{q}_{\perp 1}^{\,2}} \mathcal{F}(\mathbf{x_1}, \vec{q}_{\perp \mathbf{1}}^{\,\mathbf{2}}, \mu_{\mathbf{f}}^{\mathbf{2}}) \int \frac{d^2\vec{q}_{\perp 2}}{\pi \vec{q}_{\perp 2}^{\,2}} \mathcal{F}(\mathbf{x_2}, \vec{q}_{\perp \mathbf{2}}^{\,\mathbf{2}}, \mu_{\mathbf{f}}^{\mathbf{2}}) \times \delta^{(2)}(\vec{q}_{\perp 1} + \vec{q}_{\perp 2} - \vec{p}_\perp) \frac{\pi}{(x_1 x_2 s)^2} \overline{|\mathcal{M}|^2}$$

where the momentum fractions of gluons are fixed as $x_{1,2} = m_T \exp(\pm y)/\sqrt{s}$.

The off-shell matrix element (we restore the color-indices):

$$\mathcal{M}^{ab} = \frac{q_{1\perp}^\mu q_{2\perp}^\nu}{|\vec{q}_{\perp 1}||\vec{q}_{\perp 2}|} \mathcal{M}^{ab}_{\mu\nu} = \frac{q_{1+} q_{2-}}{|\vec{q}_{\perp 1}||\vec{q}_{\perp 2}|} n^+_\mu n^-_\nu \mathcal{M}^{ab}_{\mu\nu} = \frac{x_1 x_2 s}{2|\vec{q}_{\perp 1}||\vec{q}_{\perp 2}|} n^+_\mu n^-_\nu \mathcal{M}^{ab}_{\mu\nu}\,.$$

In covariant form, the matrix element reads:

$$\mathcal{M}^{ab}_{\mu\nu} = (-i) 4\pi\alpha_s\, \varepsilon_{\mu\nu\alpha\beta} q_1^\alpha q_2^\beta \frac{Tr[t^a t^b]}{\sqrt{N_c}}\, I(\vec{q}_{\perp 1}^{\,2}, \vec{q}_{\perp 2}^{\,2})\,.$$

Unintegrated gluon densities

$$xg(x,\mu_f) \propto \int^{\mu_F} dk_\perp^2 \frac{\mathcal{F}(x,k_\perp^2,\mu_F^2)}{k_\perp}$$

Figure:
Unintegrated gluon densities at scale $\mu_F^2 = 100\,\mathrm{GeV}^2$ typical for $\eta_c(1S)$ production in proton-proton collisions.

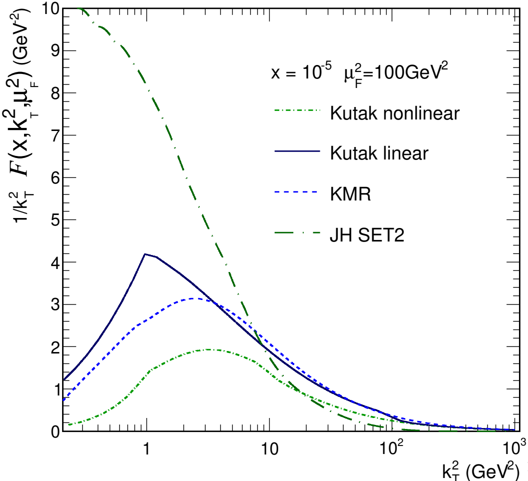

LHCb kinematics $2 < y < 4.5$, $p_T > 6.5\mathrm{GeV}$

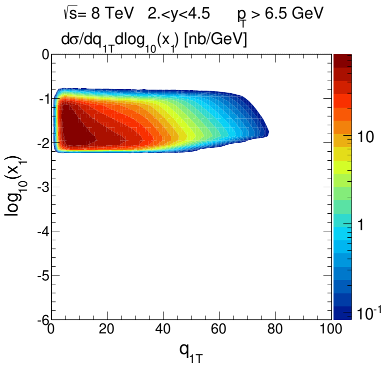

Figure: Distributions in gluon transverse momentum: q_{1T} or q_{2T} and the logarithm of the momentum fraction: $\log_{10}(x_1)$, $\log_{10}(x_2)$

prompt $pp \to \eta_c(1S)$ - different potential models

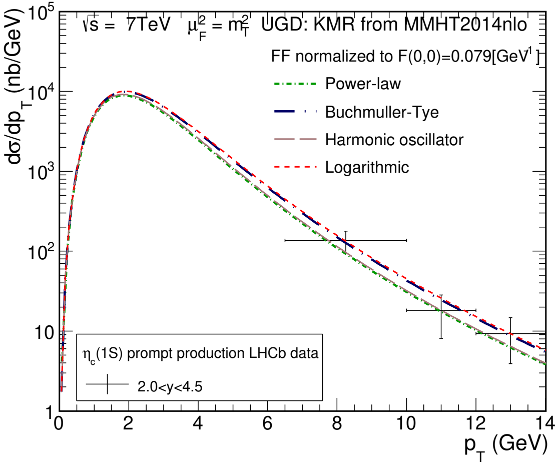

Figure: Differential cross-section in transverse momentum of the meson η_c (1S) for different potential models (I. Babiarz, R. Pasechnik, W. Schäfer, A. Szczurek *JHEP* **02**, 037(2020))
LHCb Collaboration R. Aaij et al., Eur.Phys.J.C 75 (2015) 7, 311, 1409.3612 [hep-ex]

prompt $pp \to \eta_c(1S)$

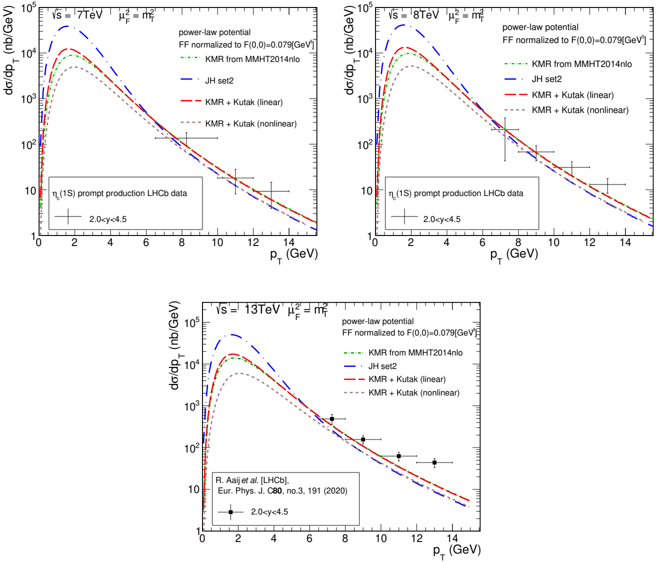

Figure: data: LHCb Collaboration, R. Aaij et al., Eur.Phys.J.C 75 (2015) 7, 311
LHCb Collaboration, R. Aaij et al., Eur.Phys.J.C 80 (2020) 3, 191

prompt $pp \to \eta_c(2S)$

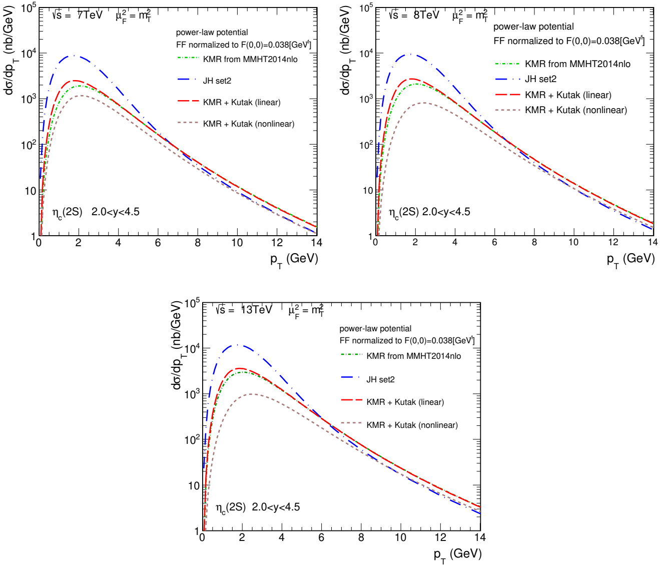

Figure: Differential cross-section as a function of η_c (2S) transverse momentum for $\sqrt{s} = 7,\, 8\,TeV$ (top inlays) and $13\,\mathrm{TeV}$ (bottom).

Conclusions

- The transition form factor for different wave functions obtained as a solution of the Schrödinger equation for the $c\bar{c}$ system for different phenomenological $c\bar{c}$ potentials from the literature, was calculated.
- We have studied the transition form factors for $\gamma^*\gamma^* \to \eta_c$ (1S,2S) for two space-like virtual photons, which can be accessed experimentally in future measurements of the cross section for the $e^+e^- \to e^+e^-\eta_c$ process in the double - tag mode.
- The transition form factor for only one off-shell photon as a function of its virtuality,was studied and compared to the BaBar data for the $\eta_c(1S)$ case.
- Dependence of the transition form factor on the virtuality was studied and the delayed convergence of the form factor to its asymptotic value $\frac{8}{3}f_{\eta_c}$ as predicted by the standard hard scattering formalism, was presented.
- There is practically no dependence on the asymmetry parameter ω, which could be verified experimentally at Belle 2.